Evaluation of 6.5-kV SiC PiN Diodes in a Medium-Voltage, High-Power 3L-NPC Converter

Felipe Filsecker, Rodrigo Alvarez, Steffen Bernet

***Abstract*—This work is focused on evaluating the advantages of 6.5-kV SiC PiN diodes in a 4.16-kV, 8-MVA Neutral Point Clamped (NPC) Voltage Source Converter (VSC). Electrothermal models of the power semiconductors are elaborated based on measurement data of a SiC diode module prototype, as well as of commercial Si devices. These models are integrated into a converter simulation, where the junction temperatures of each device are used to determine the maximum power output under different device configurations. For the analysis, a parallel connection of two 6.5-kV IGBTs as well as a series connection of two 3.3-kV IGBTs are considered as switches. The influence of the current change rate during the IGBT turn-on is also studied. SiC PiN diodes are used as a replacement for the NPC diodes of the converter and as antiparallel diodes in IGBT modules. The results obtained indicate that an increase of the output power by 17% can be achieved using SiC NPC diodes for the studied current change rates. Alternatively, for a constant output power, the switching frequency of the converter can be increased by 69%, reducing the converter size and system costs by the use of smaller filters.**

I. Introduction

SiC power devices are nowadays subject of extensive investigation, as they enable new, attractive fields for power electronics, such as high temperature, high frequency and high power density operation. The analysis presented here has been focused on medium-voltage megawatt-range converters, where until now Si-based devices are exclusively used [1]. Recent developments targeting this field include very high voltage (10–12 kV) active devices (IGBT, MOSFET) [2], [3], switches with antiparallel diodes, either in Si-SiC hybrid technology [4] or completely based on SiC [5], PiN diodes [6]–[9] and junction barrier Schottky (JBS) diodes [10], among others.

The publications cited above show that the preferred SiC rectifier structures for the medium-voltage range are JBS and PiN. As stated in [11], traditional Schottky barrier diodes have the drawback of a prohibitively large on-state resistance at high blocking voltages (> 2.5 kV). JBS and PiN diodes use the effect of bipolar conduction mode to achieve low resistance values. The drawbacks of diodes operating in bipolar conduction mode are larger reverse recovery losses and a high knee voltage due to to the wide bandgap of SiC [12]. These problems, however, are not so critical as the consequences that crystal defects have in these devices. Bipolar devices are prone to forward voltage drift due to basal plane dislocations in the SiC substrate, which is one of the main hurdles in the development of reliable devices [13].

To assess the potential of a new device it is necessary to evaluate its performance in the converter. For voltage source converters (VSC), recent attention has been directed to the popular 3-Level Neutral Point Clamped (3L-NPC) topology with 6.5- and 10-kV devices and the 2-level converter topology with 10-kV devices, for an output power of 1 MW [14] and 100 kVA [15]. Both papers present comparisons with Si-based converters by using device models scaled from die-level measurements with currents below 10 A. The analysis is focused on converter losses, efficiency and high-frequency operation; thermal calculations have not been included.

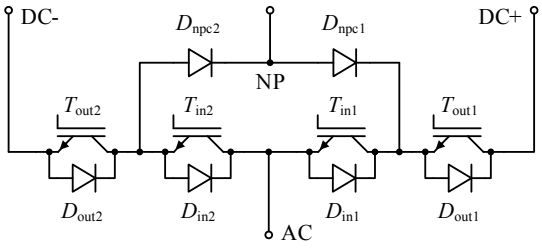

Fig. 1. Neutral-Point Clamped (NPC) converter topology, one phase.

In this paper, a comparison at converter level is presented, but with a different approach. The starting point is the 6.5-kV, 1-kA SiC PiN diode module already presented in [16], [17]. The prototype tested contains 80 dies, packaged in an industry-standard $130 \times 140\,\text{mm}^2$ module. The next version – not tested yet– contains 120 dies in a $190 \times 140\,\text{mm}^2$ module with a current rating of 1.5 kA. This version (6.5 kV, 1.5 kA, 120 dies) was considered as the basis for the converter design. The new module has also been thermally characterized, which allows the calculation of the junction temperature.

The 3L-NPC VSC topology was chosen for the comparison, see Fig. 1 for the diagram of one phase-leg. Currently, a series connection of two 3.3-kV IGBT modules for the switches and two 3.3-kV diodes for the NPC positions with a current rating of 1500 A are the preferred solution in industrial IGBT-based converters with an output power of about 7–8 MVA [18].

The potential of using SiC technology in 3L-NPC converters was already experimentally investigated on a lower scale (230 V, 10 kVA) in [19], where a loss reduction of 10% compared to the Si counterpart was achieved. However, these results are not easy to scale to medium-voltage, high-power applications. This paper contributes with a measurement-based estimation of the advantages of SiC PiN diodes in this field. For this purpose, several device configurations at different current change rates were investigated for the NPC converter, such as 3.3- and 6.5-kV IGBT modules, SiC diodes as NPC and as antiparallel diodes inside the IGBT modules.

II. Power Device Modeling

In order to evaluate the performance of a given power semiconductor setup in a converter it is mandatory to calculate the junction temperature for each device under worst-case conditions. The key to an accurate temperature estimation is a model of the power device that reflects the losses under conditions that resemble the ones in the final application.

Electrothermal models based on ideal devices and on accurate approximations of measured on-state voltages and switching losses, due to their simplicity, accuracy and higher simulation speed, were preferred over physical or behavioral device models for the junction temperature estimation. A look-up table containing measured on-state voltages and switching losses assigns the losses according to the simulated voltage and current waveforms to each device. Using thermal resistance values, the device junction temperatures are calculated in a closed loop at each simulation step. This means that the temperature-dependent losses change the device junction temperature, which is used to adjust the losses in the next simulation step. The implementation is done with the simulation software PLECS, which includes all the features needed for this purpose [20].

The device models of this work were elaborated using the following procedure:

- For commercial devices the on-state voltage was extracted out of the datasheet. In the case of the SiC diode, where no datasheet is available, the on-state characteristic was measured in one of the module prototypes as shown in [17].
- Switching losses are highly sensitive to external conditions, such as the stray inductance and the GDU, and also to internal conditions, such as the junction temperature and the commutation voltage. In order to obtain comparable loss characteristics, a test bench was elaborated and the different device pairs were switched under equal conditions, see [17], [21] for an example of measurements performed with 6.5-kV devices. The 3.3-kV devices were measured in an analogous manner. The integration limits in the voltage and current waveforms for the loss calculation were set as suggested in [22].
- Thermal resistances of the commercial devices were taken from the datasheet. In the case of the SiC diode module, these values were estimated with simulations of the physical structure. Tab. I lists the values for each device.

The switching losses of the 6.5-kV IGBTs used in the models for the simulations here presented were calculated out of measurements done with a new fully digitally controlled GDU [23], which does not rely on gate resistors for adjusting the switching speed. The 3.3-kV series-connected IGBTs were driven with a traditional analog GDU used in commercial converters. Both GDUs operate with gate-emitter voltages of –10/+15 V. In order to keep both device measurement sets and models apart, the device configurations related to the 6.5-kV IGBTs use the *R65* prefix and the ones related to the 3.3-kV devices use *R33*. The models analyzed in this paper include two different switching speeds for 3.3-kV devices and three for 6.5-kV devices. The switching speeds for the IGBT turn-on transients were labeled as *di/dt1*, *di/dt2* and *di/dt3*, Fig. 2 presents detailed values for each configuration. The reference speed used with Si devices is labeled as *R65 Si* or *R33 Si* depending on the voltage class and is equal or close to the corresponding *di/dt1* speed.

TABLE I
Thermal Resistances

Device (K/kW)	$R_{\text{th,j-h}}$	$R_{\text{th,h-a}}$
FZ600R65KF2 IGBT	20.1	
FZ600R65KF2 diode	38.5	15.0
SiC-D-40	47.7	
FZ1500R33HL3 IGBT	18.5	15.0
FZ1500R33HL3 diode	25.5	
DD600S65K1 (full mod.)	18.5	21.9
DD1000S33 (full mod.)	19.25	21.9
SiCD-120	15.9	15.0

$R_{\text{th,j-h}}$: Thermal resistance, junction to heat sink
$R_{\text{th,h-a}}$: Thermal resistance, heat sink to ambient

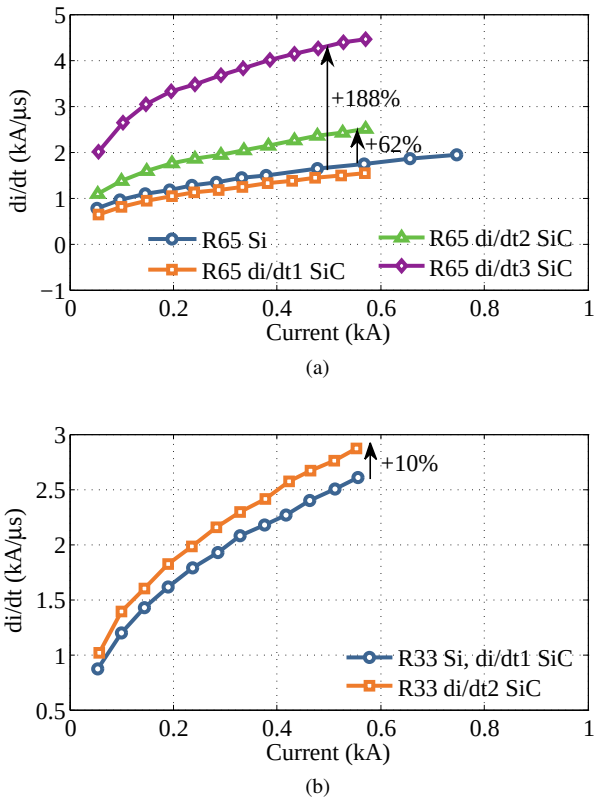

Fig. 2. Current slope di/dt for IGBT turn-on transients at 2.9 kV and 75°C. R65: IGBT FZ600R65KF2 (single), R33: IGBT FZ1500R33HL3 (series connection of two devices). The slope was evaluated between 50% of the commutated current value and 50% of the reverse recovery maximum value of the diode turn-off current waveform.

As an example, switching waveforms of the SiC PiN diode for *R65 di/dt1*, *R65 di/dt3* and *R33 di/dt2* are shown in Fig. 3. Special attention was paid to the high-frequency oscillations caused by the SiC diode [17]. In order to turn off the diode at a high di/dt, the oscillations were dampened with an *RC* snubber, refer to [24] for details. The on-state characteristics and the switching loss approximations of the 6.5-kV, 1.5-kA SiC NPC diode as used in the converter simulations can be

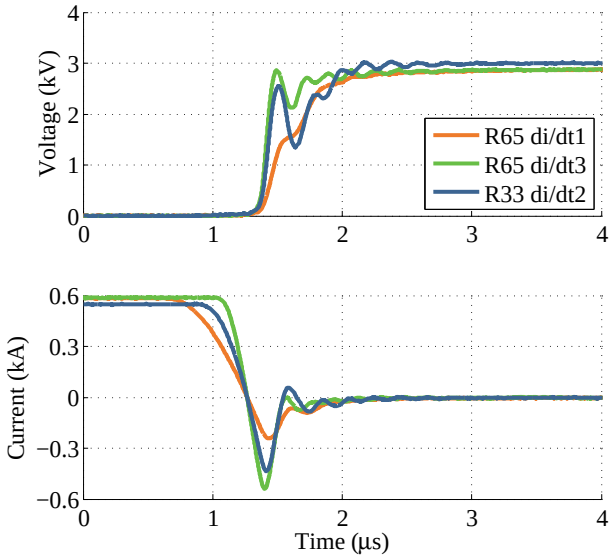

Fig. 3. Voltage and current waveforms of the 6.5-kV, 1-kA SiC diode module turn-off transients for three different configurations. (R65: IGBT FZ600R65KF2, R33: 2× IGBT FZ1500R33HL3 V_{dc} = 2.9 kV, I_D = 0.6 kA, T_j = 75°C, *RC* snubber: 9.4 nF, 4.7 Ω for *R65 di/dt1, R33 di/dt2* and 14.1 nF, 4.7 Ω for *R65 di/dt3*)

seen in Fig. 4.

The models of the SiC diode required some scaling in order to estimate the on-state voltage v_F and switching losses E_{sw} out of a module prototype containing n_1 dies to one containing n_2 dies. These were scaled linearly, considering equal current distribution among the dies:

$$v_F(n_2) = \frac{n_1}{n_2} v_F(n_1) \tag{1}$$

$$E_{sw}(n_2) = \frac{n_2}{n_1} E_{sw}(n_1) \tag{2}$$

III. Determination of Maximum Converter Rating

One of the most important criteria for the evaluation of a certain device configuration is the maximum converter power. In the majority of industrial applications the maximum converter power is limited by the maximum device junction temperature at worst-case conditions. 3L-NPC converters have an unequal junction temperature distribution among their devices. The four critical operating points (OPs) are at maximum or minimum modulation depth m_a, and at a $\cos\varphi$ of 1 or −1, as indicated in [25] and summarized in Table II.

For each critical point, either the IGBTs or the diodes of one position (*in*, *out* or *npc* in Fig. **??**) per phase leg have the highest junction temperature. Not all of the points listed in that table are critical for every application. In the case of quadratic torque loads, the most critical point is OP1. If the load is regenerative, OP2 is also of interest. Considering that these loads are usually operated with a V/Hz control (output voltage increases linearly with the output frequency), at low modulation depths the current required by the load is also very low, which is why OP3 and OP4 are not critical.

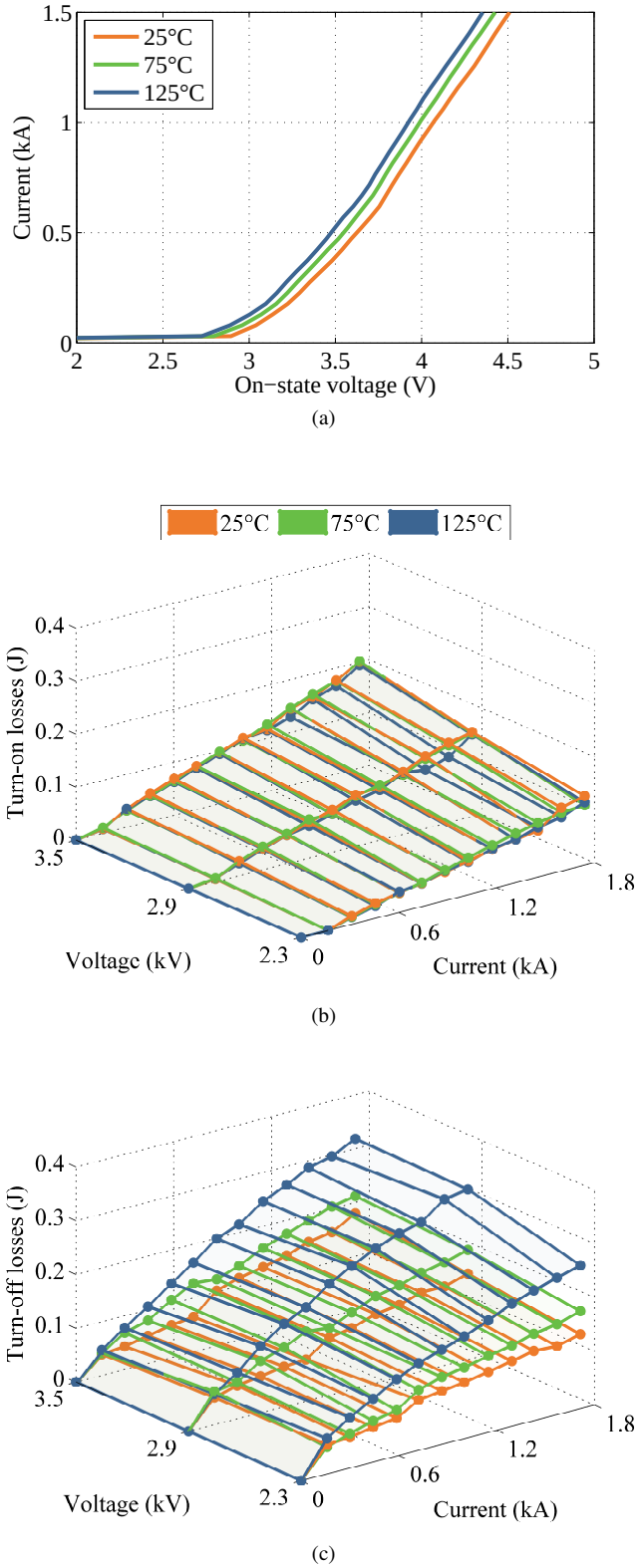

Fig. 4. Approximation of on-state characteristic and switching losses of the 6.5-kV, 1.5-kA SiC PiN diode module (120 dies) switched with IGBT FZ600R33KF2: (a) on-state characteristics, (b) turn-on losses, (c) turn-off losses, $R_{th,j\text{-}h}$ = 15.9 K/kW.

In the case of loads with constant torque the points OP3 and OP4, representing nominal load current at zero speed

TABLE II
CRITICAL OPERATING POINTS FOR 3L-NPC VSC

	OP1	OP2	OP3	OP4
m_a	max. (1.15)	max. (1.15)	min. (0.01)	min. (0.01)
$\cos\varphi$	1 (mot.)	–1 (gen.)	1 (mot.)	–1 (gen.)

(output frequency very low), are critical. In an NPC VSC, the inner switches T_{in} and NPC diodes D_{npc} are stressed with nominal current for long periods. The junction temperature over one cycle can increase over the maximum allowed, which is why a derating of the converter is required. Depending on the cooling conditions, this derating can amount to even 50% of the nominal power. To evaluate the converter performance in OP3 and OP4 properly, dynamic electrothermal models of the power devices are required. If the output frequency of the converter is low (e.g. < 15 Hz), the temperature ripple in the semiconductors becomes more significant than the average junction temperature. Since no dynamic thermal model of the SiC p-i-n diode module was available, the analysis that follows is done considering output frequencies of 50 Hz and quadratic torque loads, dissipative and regenerative, where only OP1 and OP2 are of interest.

IV. ANALYSIS

Different device configurations were considered for the converter simulations, see Tab. III. These can be divided into three main groups: The group *All-Si* only uses commercial Si devices, the group *SiC-NPC* considers SiC diodes for the NPC diodes D_{npc}, and the group *SiC-D* includes SiC diodes for both the NPC and the inverse diodes of the outer switches (D_{npc} and D_{out}). The use of a SiC diode in D_{in} is not presented here, as it does not provide any advantage. Contrary to the diodes D_{npc} and D_{out}, the inner diodes D_{in} in an NPC phase-leg do not experience reverse recovery losses, because the IGBT associated to it remains turned on when the current commutates. For these diodes only conduction losses are relevant. Since Si technology achieves currently better on-state characteristics and thermal resistance values for PiN diodes than SiC technology, e.g. Tab. I, the inclusion of SiC PiN diodes would be counterproductive [19]. Preliminary results of this evaluation at converter level were presented in [26], where only 6.5-kV devices and one switching speed di/dt were taken into account. The GDU used in that paper was not optimized and caused higher switching losses than the one used for this analysis.

To achieve comparable device current and voltage ratings, 6.5-kV devices were connected in parallel and 3.3-kV devices in series. In other words, the switch composed of T_{out1} and D_{out1} in Fig. 1 represents either the series connection of two 3.3-kV, 1500-A IGBT modules FZ1500R33HL3 or the parallel connection of two 6.5-kV, 600-A IGBT modules FZ600R65KF2, depending on the voltage class analyzed. The IGBT modules FZ1500R33HL3 and FZ600R65KF2 have the same footprint. For the SiC diode a special label indicates the number of parallel chips. That is, the designation *SiC-D-120* (Tab. III) means that 120 parallel dies are in one SiC diode module. In contrast, the inverse diode D_{out} has only 40 parallel dies due to space limitations inside a standard $140\times190\,\mathrm{mm}^2$ IGBT module.

TABLE III
DEVICE CONFIGURATIONS

Name	T_{in}, T_{out}, D_{in}	D_{out}	D_{npc}
R65 All-Si	FZ600R65KF2	FZ600R65KF2	DD600S65K1
R65 SiC-NPC	FZ600R65KF2	FZ600R65KF2	SiC-D-120
R65 SiC-D	FZ600R65KF2	SiC-D-40	SiC-D-120
R33 All-Si	FZ1500R33HL3	FZ1500R33HL3	DD1000S33
R33 SiC-NPC	FZ1500R33HL3	FZ1500R33HL3	SiC-D-120

FZ600R65KF2, DD600S65K1 and SiC-D-40: 2× parallel
FZ1500R33HL3 and DD1000S33HE3: 2× series
SiC-D-120: single

As mentioned in the introduction, the series connection of devices is the preferred solution for industrial 4.16-kV converters today. A symmetrical voltage distribution of the series-connected devices is achieved by an active gate voltage control with collector-emitter voltage feedback [27]. A bulky RC snubber is required for the dynamic and static balancing of the NPC diodes. The IGBTs are statically balanced by resistors. The parallel connection of 6.5-kV devices is not so popular at medium voltage applications, because 3.3-kV devices enable a higher converter power than 6.5-kV devices [1]. Depending on the physical converter layout, the design for a symmetrical current distribution of parallel devices can be as complex as the methods for a symmetrical voltage distribution of series-connected devices. However, newly developed algorithms that solve dynamic and static current sharing in a simple way have been recently reported. In [28], for example, a dynamic balancing method is implemented in the GDU, without the need of neither extra passive components nor dedicated current measurement circuits.

A 3L-NPC VSC with the parameters shown in Tab. IV was considered to determine and to compare the maximum converter power and switching frequency. The modulation implemented is a conventional sine-triangle PWM with 1/6 3rd harmonic injection. For low modulation depths (< 0.575), the reference was alternated from the upper to the lower carrier band (two-level modulation), to avoid an overheating of the NPC diodes [29]. The thermal resistance values for the heat sink $R_{th,h\text{-}a}$ correspond to a water cooling system, see the last column of Tab. I. The dc-link voltage for an output voltage of 4.16 kV corresponds to 6.2 kV; due to the 3L-NPC topology, each device switches at a voltage that is equal to 3.1 kV. This explains the voltage at which the devices where characterized (2.3…3.5 kV).

A. SiC diode as NPC diode

The main advantage of using a SiC diode as NPC diode D_{npc} is the switching loss reduction in the T_{out} IGBTs. (Refer to [30] for details about the commutations in a 3L-NPC phase leg.) This leads to a lower junction temperature in the device that enables a higher output power in the converter. Additionally, it is possible to increase the di/dt during T_{out} turn-on transients to achieve an additional loss reduction. With current Si devices,

TABLE IV
CONVERTER SETUP

Dc-link voltage		6.2 kV
Output voltage		4.16 kV
Output frequency		50 Hz
Switching frequency		465 Hz
Output current		1000 A
Cooling water temperature		50°C
Max. avg. junction temp.		120°C
Stray inductance		245 nH
Min. turn-on time	R65	100 µs
	R33	25 µs

the switching speed of the IGBT at turn-on is limited by the reverse blocking safe operating area (RBSOA) of the diode.

It is important to note that for this configuration (*SiC-NPC*), the diodes D_{out} are standard Si diodes. This means that the current slope di/dt in the T_{in} IGBTs, which commutate with the D_{out} diodes, should not be increased. Hence, the setup *R65 SiC-NPC di/dt2* stands for an NPC phase leg with 6.5-kV devices, as in Tab. III, where only the T_{out} IGBTs are turned on at a higher speed, see Fig. 2. The T_{in} IGBTs switch at the standard speed for Si devices.

Figure 5a shows the maximum converter output power for three different di/dt using paralleled 6.5-kV devices. As a reference, the *All-Si* configuration is included. The cases of unidirectional (only OP1) and bidirectional (OP1 & OP2) energy flow are evaluated. The use of SiC diodes as NPC diodes allows an increase of at least 13% in the output power. This is a consequence of the lower switching losses in T_{out}, as shown in Fig. 6a, where the device loss and temperature distribution for OP1 is analyzed.

Increasing the IGBT turn-on di/dt has only marginal influence on the output power. Considering a di/dt increase of 188% (from *di/dt1* to *di/dt3*) and unidirectional energy flow, a 4% higher output power can be achieved (from 8.58 to 8.96 MVA). For bidirectional energy flow, the additional switching speed does not translate into a higher output power. This is so because for higher di/dt (*didt2*, *didt3*), the limiting device in the converter changes from T_{out} to D_{in}, on which the SiC NPC diode does not have any influence, compare T_{out} in Fig. 6a and D_{in} in Fig. 6b.

B. SiC diode as antiparallel diode

The next step after replacing the NPC diodes by SiC diodes would be to integrate this technology in a hybrid Si-IGBT/SiC-diode module, similar to the work of Takao *et al.* [4]. Using the data collected from the measurements of the FZ600R65KF2 and the SiC diode modules, a hybrid module containing the 6.5-kV 600-A IGBT and an antiparallel SiC PiN diode made of 40 dies was modeled and used in the converter simulations, see *R65 SiC-D* in Tab. III.

The results for maximum converter output power are shown in Fig. 5b. For unidirectional current flow, the D_{out} diodes do not play any role in defining the maximum power, since T_{out} is the limiting device position. For bidirectional converters, compare with Fig. 5a, the antiparallel SiC diodes have a negative effect. The source of this behavior can be clearly appreciated by comparing Figs. 6b and 7. The losses in D_{out} are

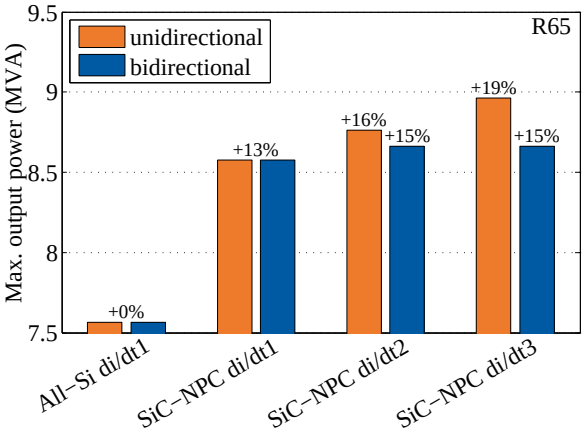

(a)

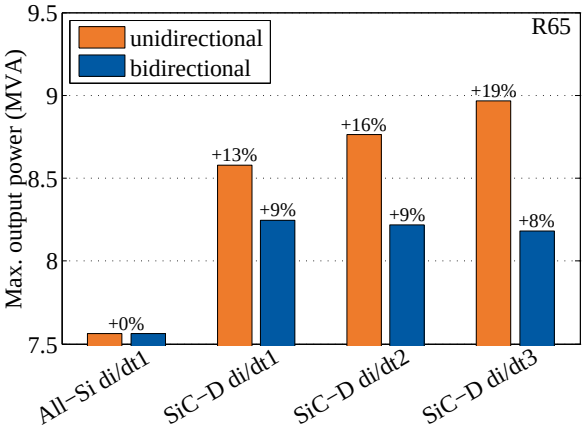

(b)

Fig. 5. Maximum converter output power for the NPC converter with 2 parallel-connected 6.5-kV IGBTs as switches: (a) *R65 SiC-NPC* and (b) *R65 SiC-D* device configurations at different di/dt compared to *R65 All-Si*, considering unidirectional (OP1) and bidirectional (OP1 & OP2) energy flow. (f_{sw} = 465 Hz, V_{dc} = 6.2 kV)

not reduced, but increased, mostly due to the higher on-state voltage of the SiC PiN diodes. Moreover, the SiC diode has a 24% higher thermal resistance value between junction and case $R_{\text{th,j-c}}$. As a consequence, the junction temperature of this diode is considerably higher, as Fig. 7 demonstrates, limiting the output power of the converter. One possible solution to this would be to take advantage of the high temperature operation of the SiC diode. In the prototype analyzed here, the maximum junction temperature allowed is 125°C, due to limitations in the module assembly technology. Moreover, enabling high temperature operation in a hybrid package containing Si and SiC dies with different maximum junction temperatures is a challenge for the packaging technology.

C. SiC NPC diode with 3.3-kV Si IGBTs

The SiC diode module was also investigated in combination with a series connection of two 3.3-kV IGBTs FZ1500R33HL3. The maximum converter output power for

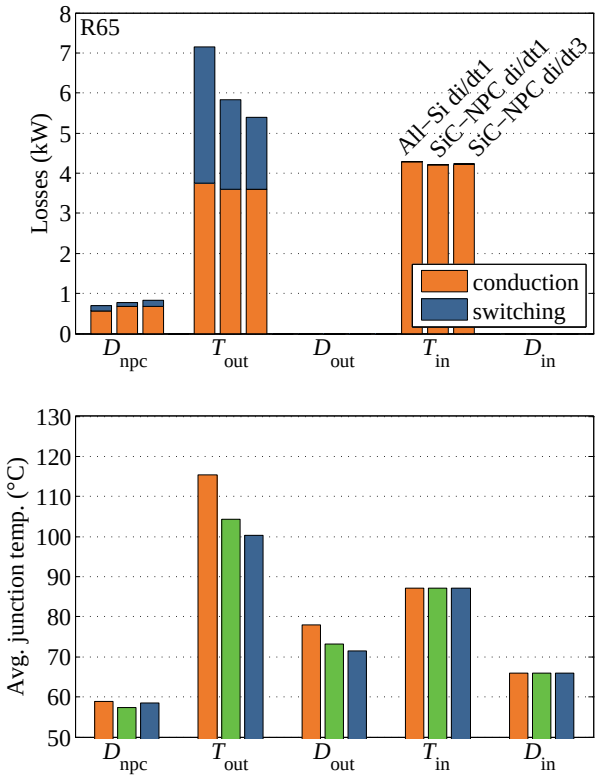

(a) OP1: m_a = 1.15, $\cos\varphi$ = 1

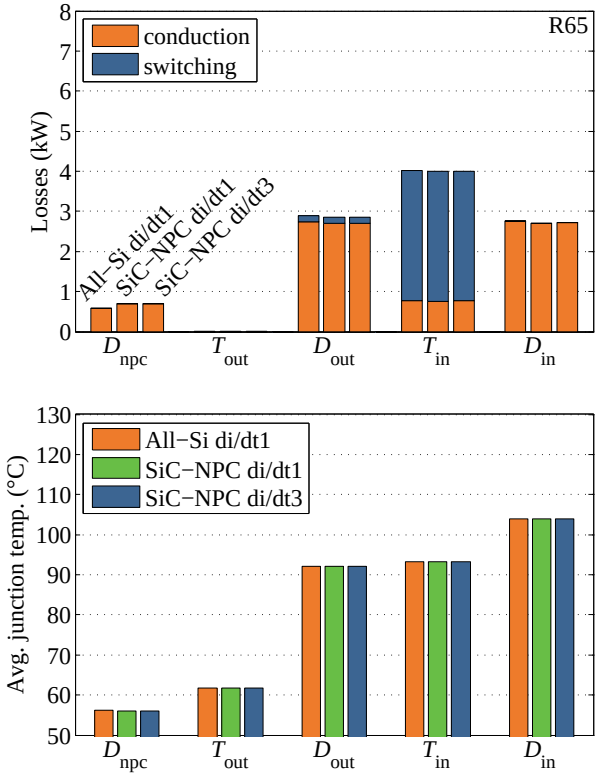

(b) OP2: m_a = 1.15, $\cos\varphi$ = –1

Fig. 6. Total conduction and switching losses and average junction temperature distribution among each device group for *R65 SiC-NPC* compared to *R65 All-Si* device configuration. (I_{out} = 1000 A, f_{sw} = 465 Hz, V_{dc} = 6.2 kV)

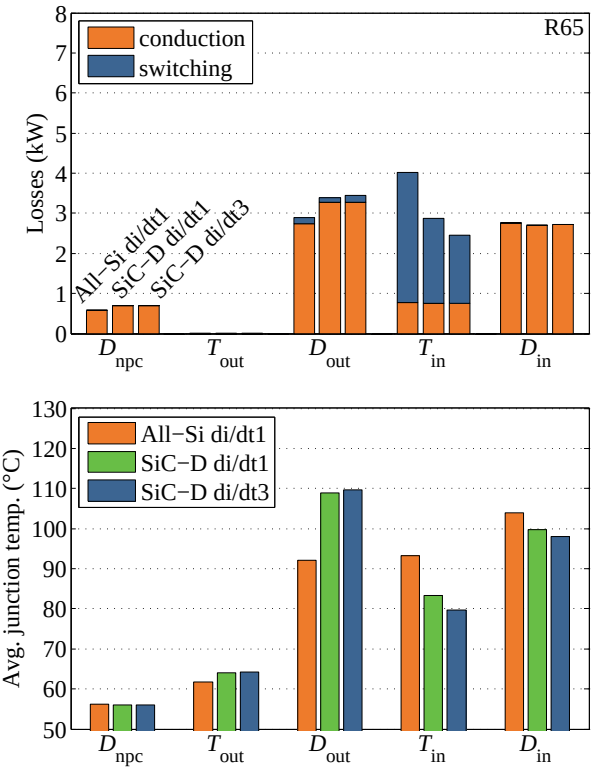

Fig. 7. Total conduction and switching losses and average junction temperature distribution among each device group for *R65 SiC-D* compared to *R65 All-Si* device configuration at OP2: m_a = 1.15, $\cos\varphi$ = –1. (I_{out} = 1000 A, f_{sw} = 465 Hz, V_{dc} = 6.2 kV)

the configurations *R33 All-Si* and *R33 SiC-NPC* can be seen in Fig. 8. For this set of configurations, the power rating depends only on OP1, in both uni- and bidirectional cases. For the same di/dt the SiC NPC diode allowed an output power increase of 16% compared to the *All-Si* configuration. By turning on the IGBT at *di/dt2* (+10% compared to *di/dt1*), only a marginal increase of the output power can be achieved (+1%). Fig. 9 illustrates the loss and temperature distribution among the devices in the most critical point (OP1).

D. Best semiconductor configurations

The best device configurations analyzed in the paper are summarized in Fig. 10, for maximum converter output power as well as maximum switching frequency. An increase of 10% to 17% of the output power has been determined. Alternatively, the SiC diode performance can be used to increase the switching frequency by 41 to 69%. By comparing the cases *R33 SiC-NPC di/dt2* and *R65 SiC-NPC di/dt3* the advantages of using 3.3-kV devices can be appreciated. Although the current change rate *R33 di/dt2* is considerably lower than *R65 di/dt3* (≈–36%, see Fig. 2), the 3.3-kV device configuration achieves a higher output power. Better results could be achieved by increasing the di/dt to higher levels than the ones used here, as long as the overvoltages, oscillations and dv/dt values are acceptable.

Figure 11 indicates the efficiency of the 3L-NPC converter, depending on the device configuration used. For this cal-

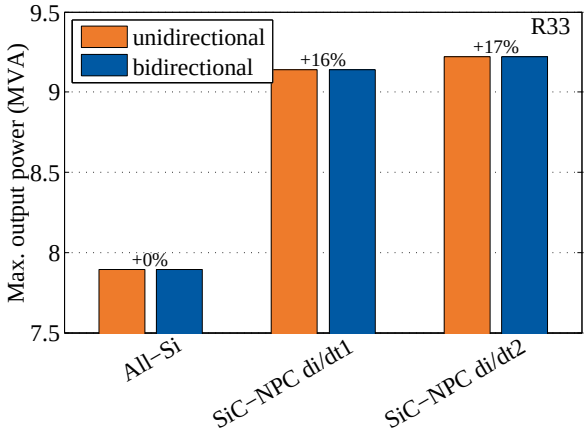

Fig. 8. Maximum converter output power for an NPC converter with a series connection of two 3.3-kV IGBTs as switches, considering unidirectional (OP1) and bidirectional (OP1 & OP2) energy flow. (f_{sw} = 465 Hz, V_{dc} = 6.2 kV, $T_{j,max}$ = 120°C)

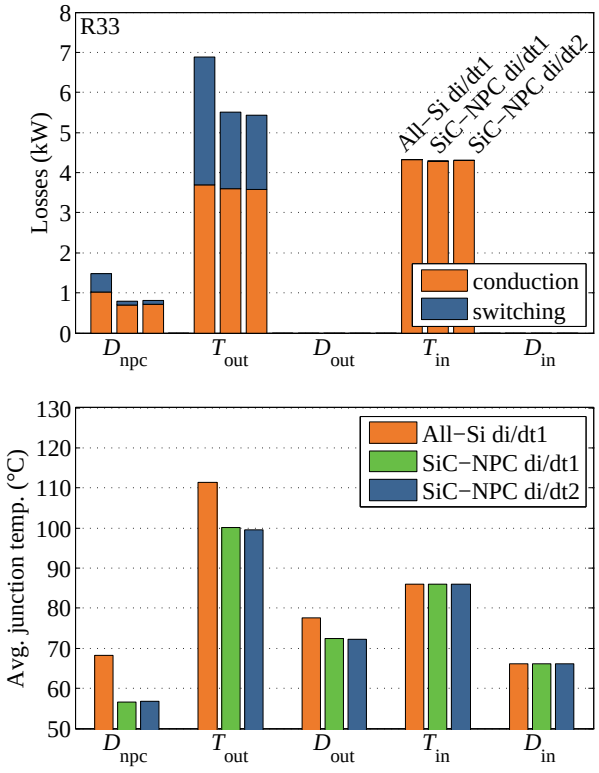

Fig. 9. Total conduction and switching losses and average junction temperature distribution among each device group for *R33 SiC-NPC* compared to *R33 All-Si* device configuration at OP1: m_a = 1.15, cos φ = 1. (I_{out} = 1000 A, f_{sw} = 465 Hz, V_{dc} = 6.2 kV)

culation, the effect of RC snubbers and resistors for static balancing, in the case of the 3.3-kV IGBT configuration, was considered. For the current balancing of the parallel-connected 6.5-kV devices, non-dissipative balancing algorithms have been assumed [28].

Three different efficiency levels can be clearly distinguished. The lowest efficiency is achieved by the *R33 All-Si di/dt1*

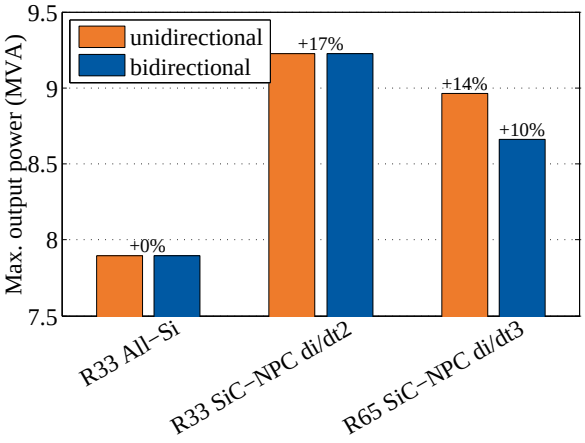

(a)

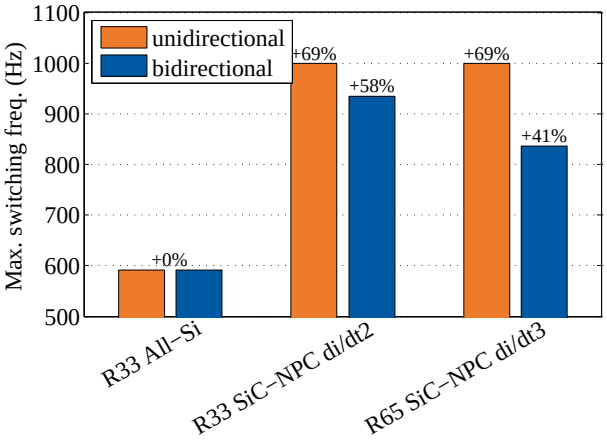

(b)

Fig. 10. Maximum converter output power (a) and switching frequency (b) for an NPC converter with the best semiconductor configurations analyzed, considering unidirectional (OP1) and bidirectional (OP1 & OP2) energy flow. (f_{sw} = 465 Hz (a), I_{out} = 1000 A (b), V_{dc} = 6.2 kV, $T_{j,max}$ = 120°C)

configuration, which is mainly determined by the resistors needed for static voltage sharing (11 kΩ/device). The combination *R33 SiC-NPC di/dt2* has a better performance, since the NPC diodes do not require an additional circuit for static balancing. The highest efficiency is reached by 6.5-kV devices, where no extra elements are needed for balancing purposes. The small RC snubber required for the diode switching (9.4–14.1 nF, 4.7 Ω) has a negligible impact on the efficiency. The difference between *R65 All-Si di/dt1* and *R65 SiC-NPC di/dt3* is very low (≈0.05%) and cannot be appreciated in the picture. This is related to the low switching frequency used in the characteristic example for industrial applications (465 Hz).

V. Conclusions

In this paper, different semiconductor configurations considering 6.5-kV and 3.3-kV IGBTs in combination with SiC PiN diodes were investigated. In the application example of a 4.16-kV, 7-MVA 3L-NPC VSC, an increase in the output power by 10 to 17% was estimated through simulations

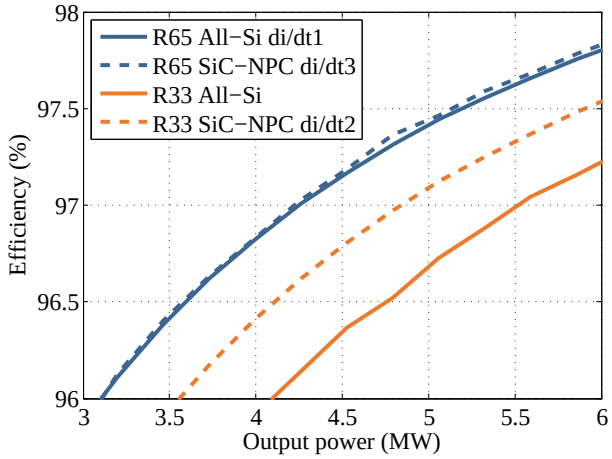

Fig. 11. Efficiency of the 3L-NPC VSC for the different device configurations. (V_{dc} = 6.2 kV, I_{out} = 1000 A, $\cos\varphi$ = 0.85, f_{sw} = 465 Hz)

with measurement-based device loss models. Alternatively, an increase in the switching frequency up to69% could be achieved. A further increase of the output power or the switching frequency could eventually be achieved by using a higher di/dt at IGBT turn-on and/or combining SiC technology with other improvements for 3L-NPC converters, such as the Active NPC (ANPC) topology [25], [30].

The best device configuration consists of SiC diodes in the NPC positions with the outer IGBTs (T_{out} in Fig. 1) turning on with an increased di/dt and the inner IGBTs T_{in} at normal speed. The switches can be either parallel-connected 6.5 kV or series-connected 3.3-kV IGBTs. The parallel connection, due to the absence of passive balancing circuits, achieves a higher efficiency. The series connection, however, achieves a higher output power and is definitely superior for converters with bidirectional energy flow. A replacement of the inverse Si diodes inside the IGBT modules by SiC PiN diodes does not lead to a better performance regarding the maximum output power or the switching frequency. In terms of efficiency, for the studied switching frequency (465 Hz), the influence of the SiC PiN diodes is marginal compared to that of the balancing circuits for the 3.3-kV devices.

The attractiveness of SiC PiN diodes could be increased in the future by new packaging technologies enabling higher junction temperatures, higher robustness (power and thermal cycling) and lower thermal resistances. Furthermore, improvements in the SiC bulk material and the SiC diode design process are important next steps to increase the competitiveness of medium voltage SiC diodes [31].

Currently the SiC technology is a relatively new player in field of medium-voltage, high-power applications. Up to now, only a few working module prototypes have been elaborated and tested. This work contributes to the better understanding of the potentials and limitations of the currently available medium voltage SiC diode technology.

Acknowledgements

This work was financially supported by the German Federal Ministry of Education and Research (BMBF) under the grant number FKZ 16N10893.

References

[1] M. Hiller, R. Sommer, and M. Beuermann, "Medium-voltage drives," *IEEE Ind. Appl. Mag.*, vol. 16, no. 2, pp. 22–30, Mar. 2010.

[2] M. K. Das, C. Capell, D. E. Grider, R. Raju, M. Schutten, J. Nasadoski, S. Leslie, J. Ostop, and A. Hefner, "10 kV, 120 A SiC half H-bridge power MOSFET modules suitable for high frequency, medium voltage applications," in *IEEE Energy Conversion Congress and Exposition, ECCE 2011*, Sep. 2011, pp. 2689–2692.

[3] S.-H. Ryu, C. Capell, C. Jonas, L. Cheng, M. O'Loughlin, A. Burk, A. Agarwal, J. Palmour, and A. Hefner, "Ultra high voltage (>12 kV), high performance 4H-SiC IGBTs," in *Proc. 24th Int. Symp. Power Semiconductor Devices and ICs ISPSD '12*, 2012, pp. 257–260.

[4] K. Takao, K. Wada, K. Sung, Y. Mastuoka, Y. Tanaka, S. Nishizawa, C. Ota, T. Kanai, T. Shinohe, and H. Ohashi, "4.5kV-400A modules using SiC-PiN diodes and Si-IEGTs hybrid pair for high power medium-voltage power converters," in *IEEE Energy Conversion Congress and Exposition, ECCE 2012*, Sep. 2012, pp. 1509–1514.

[5] A. Tanaka, S. Ogata, T. Izumi, K. Nakayama, T. Hayashi, Y. Miyanagi, and K. Asano, "Reliability investigation of SiC bipolar device module in long time inverter operation," in *Proc. 24th Int. Symp. Power Semiconductor Devices and ICs ISPSD '12*, 2012, pp. 233–236.

[6] A. Elasser, M. Agamy, J. Nasadoski, A. Bolotnikov, Z. Stum, R. Raju, L. Stevanovic, J. Mari, M. Menzel, B. Bastien, and P. Losee, "Static and dynamic characterization of 6.5kV, 100A SiC bipolar PiN diode modules," in *IEEE Energy Conversion Congress and Exposition, ECCE 2012*, Sep. 2012, pp. 3595–3602.

[7] S. Ogata, Y. Miyanagi, K. Nakayama, A. Tanaka, and K. Asano, "5kV class 4H-SiC PiN diode with low voltage overshoot during forward recovery for high frequency inverter," in *Proc. 23rd Int. Symp. Power Semiconductor Devices and ICs ISPSD '11*, May 2011, pp. 296–299.

[8] D. Peters, W. Bartsch, B. Thomas, and R. Sommer, "6.5 kV SiC PiN diodes with improved forward characteristics," in *Materials Science Forum*, vol. 645–648. Trans Tech Publ, Apr. 2010, pp. 901–904.

[9] Y. Tanaka, H. Ohashi, K. Sung, K. Takao, K. Wada, and T. Kanai, "Development of 6kV-class SiC-PiN diodes for high-voltage power inverter," in *Proc. 22nd Int. Symp. Power Semiconductor Devices and ICs ISPSD '10*, June 2010, pp. 213–216.

[10] T. Duong, A. Hefner, K. Hobart, S. Ryu, D. Grider, D. Berning, J. Ortiz-Rodriguez, E. Imhoff, and J. Sherbondy, "Comparison of 4.5 kV SiC JBS and Si PiN diodes for 4.5 kV Si IGBT anti-parallel diode applications," in *Proc. IEEE Applied Power Electronics Conf. and Exposition APEC'11*, March 2011, pp. 1057–1063.

[11] B. A. Hull, M. K. Das, J. T. Richmond, J. J. Sumakeris, R. Leonard, J. W. Palmour, and S. Leslie, "A 180 Amp/4.5 kV 4H-SiC PiN diode for high current power modules," in *Proc. 18th Int. Symp. Power Semiconductor Devices and ICs ISPSD '06*, 2006.

[12] A. Pérez-Tomás, P. Brosselard, J. Hassan, X. Jordà, P. Godignon, M. Placidi, A. Constant, J. Millán, and J. P. Bergman, "Schottky versus bipolar 3.3 kV SiC diodes," *Semiconductor Science and Technology*, vol. 23, no. 12, p. 125004, 2008.

[13] M. Treu, R. Rupp, and G. Solkner, "Reliability of SiC power devices and its influence on their commercialization – review, status, and remaining issues," in *Reliability Physics Symposium (IRPS), 2010 IEEE Int.*, May 2010, pp. 156–161.

[14] H. Mirzaee, S. Bhattacharya, S.-H. Ryu, and A. Agarwal, "Design comparison of 6.5 kV Si-IGBT, 6.5kV SiC JBS diode, and 10 kV SiC MOSFETs in megawatt converters for shipboard power system," in *Proc. IEEE Electric Ship Technologies Symp. (ESTS)*, 2011, pp. 248–253.

[15] S. Madhusoodhanan, K. Hatua, S. Bhattacharya, S. Leslie, S.-H. Ryu, M. Das, A. Agarwal, and D. Grider, "Comparison study of 12kV n-type SiC IGBT with 10kV SiC MOSFET and 6.5kV Si IGBT based on 3L-NPC VSC applications," in *IEEE Energy Conversion Congress and Exposition, ECCE 2012*, Sep. 2012, pp. 310–317.

[16] D. Peters, B. Thomas, T. Duetemeyer, T. Hunger, and R. Sommer, "An experimental study of high voltage SiC PiN diode modules designed for 6.5 kV / 1 kA," in *Materials Science Forum*, vol. 679-680. Trans Tech Publ, Mar. 2011, pp. 531–534.

[17] F. Filsecker, R. Alvarez, and S. Bernet, "Characterization of a new 6.5 kV 1000A SiC diode for medium voltage converters," in *IEEE Energy Conversion Congress and Exposition, ECCE 2012*, Raleigh, USA, Sep. 2012, pp. 2253–2260.

[18] C. Dietrich, S. Gediga, M. Hiller, R. Sommer, and H. Tischmacher, "A new 7.2kV medium voltage 3-Level-NPC inverter using 6.5kV-IGBTs," in *Proc. 12th European Conf. on Power Electronics and Applications EPE'07*, Sep. 2007.

[19] M. Schweizer, T. Friedli, and J. Kolar, "Comparison and implementation of a 3-level NPC voltage link back-to-back converter with SiC and Si diodes," in *Proc. IEEE Applied Power Electronics Conf. and Exposition APEC'10*, Feb. 2010, pp. 1527–1533.

[20] "PLECS v. 3.4," Zurich, Switzerland: Plexim GmbH, 2013. [Online]. Available: http://www.plexim.com/plecs

[21] F. Filsecker, R. Alvarez, and S. Bernet, "Comparison of 6.5 kV silicon and SiC diodes," in *IEEE Energy Conversion Congress and Exposition, ECCE 2012*, Raleigh, USA, Sep. 2012, pp. 2261–2267.

[22] "Industrial IGBT modules: Explanation of technical information," Application Note AN 2011-05 V1.1, Infineon Technologies, May 2013.

[23] K. Handt, H. Khler, M. Hiller, and R. Sommer, "Fully digitally controlled gate drive unit for high power IGBTs," in *Proc. PCIM Europe*, Nuremberg, Germany, May 2012.

[24] F. Filsecker, R. Alvarez, and S. Bernet, "Investigation of oscillations in a 6.5-kV, 1-kA SiC diode module," in *Proc. 15th European Conf. on Power Electronics and Applications EPE'13 ECCE Europe*, Lille, France, 2013.

[25] T. Brückner and S. Bernet, "Loss balancing in three-level voltage source inverters applying active NPC switches," in *Proc. IEEE Power Electronics Specialists Conf. PESC 2001*, vol. 2, 2001, pp. 1135–1140.

[26] F. Filsecker, R. Alvarez, and S. Bernet, "Investigation of a 6.5-kV, 1-kA SiC diode module for medium voltage converters," *Power Electronics, IEEE Transactions on*, 2014, to be printed.

[27] M. Bruckmann, R. Sommer, M. Fasching, and J. Sigg, "Series connection of high voltage IGBT modules," in *Proc. IEEE Industry Applications Society Annual Meeting IAS '98*, vol. 2, 1998, pp. 1067–1072.

[28] R. Alvarez and S. Bernet, "A new delay time compensation principle for parallel connected IGBTs," in *IEEE Energy Conversion Congress and Exposition, ECCE 2011*, Sep. 2011, pp. 3000–3007.

[29] T. Brückner and D. G. Holmes, "Optimal pulse-width modulation for three-level inverters," *IEEE Trans. Power Electron.*, vol. 20, no. 1, pp. 82–89, Jan. 2005.

[30] T. Brückner, S. Bernet, and H. Guldner, "The active NPC converter and its loss-balancing control," *IEEE Trans. Ind. Electron.*, vol. 52, no. 3, pp. 855–868, Jun. 2005.

[31] K. Shenai, M. Dudley, and R. F. Davis, "Current status and emerging trends in wide bandgap (WBG) semiconductor power switching devices," *ECS Journal of Solid State Science and Technology*, vol. 2, no. 8, pp. N3055–N3063, Jul. 2013.